Chapter 5

Electronic properties of single ZnO nanorod device

5-1 Single Nanorod Device

There have been extensive efforts on ZnO nanorods synthesis, but much less on the transport properties and control of electron density by external field gating. [71]–[73] In particular, there has been little done on producing single nanorod devices to demonstrate the ability to manipulate current in ZnO nanorods. The single nanorod devices properties study is important as the base of usages. we have synthesized well separated ZnO nanorod arrays on Si substrate. It is of great interest because it is an important step towards realizing single nanorod device devices. Herein, the study on interfacial properties is also important. Therefore, the junction properties of single ZnO nanorod are very important. Although the Schottky junction of Pt/ZnO and Au/ZnO has been investigated and demonstrated the ability to manipulate current in ZnO nanostructures [173][127]. Up to date, only little research has been performed on heterojunction between single nanorods with Si substrate [174].

ZnO can be used as a low-energy photon window, transmitting the photons to reach the substrate because the light transmittance of the semiconducting ZnO films generally exceeds 80% beyond the wavelength of the absorption edge [175]. If the substrate is a arrow-band-gap semiconductor, the low-energy photons will be collected

at the semiconducting substrate material, such as Si, after being transmitted through the ZnO. Since semiconducting ZnO is n-type, n-ZnO deposited on p-Si can provide a built-in potential in the p-Si side, which is the source of photoelectric effects. This is the good application of heterojunction.

ZnO/Si heterostructures, which are fabricated by utilizing the combined advantages of the large excitonic binding energy of the ZnO thin film and the cheap Si substrates are particularly interesting due to their many possible applications for optoelectronic devices operating in the blue region of the spectrum [111]. Since the optical and the electronic properties of the ZnO/Si heterostructures are very important for fabricating electronic and optoelectronic devices, systematic studies of the physical properties of ZnO thin films and ZnO/Si heterostructures are necessary for achieving high-performance devices.

In this section, we study on the electrical properties of n-ZnO/p-Si heterojunction. By using the Au coated AFM tip, I-V and C-V characteristics for both the schottky of Au/ZnO and heterojunction of ZnO/Si substrate are discussed. Finally, the frequency response of the FED with single ZnO nanorod on Si substrate was calculated.

5-2 AFM and SCM Measurement

The site-specific substrate and growth of ZnO nanorods were described in chapter 3. Topography and I-V characteristic curve measurements of heterojunction diodes were carried out using an atomic force microscope system [176]. For both measurements, a sharpened pyramidal Au-coated conducting tip with a spring constant of 0.12 N/m was employed. The surface morphology were examined by a contact mode atomic force microscopy (AFM) at a low contact force less than 10 nN in preventing possible damage of probe tips and samples. Both of the topography and electrical measurements were performed using the same tip. For I –V measurements, current was measured at various bias voltages applied between the conducting tip and contact layers using current sensing module. All measurements were performed at room temperature.

The images taken by FESEM in Fig. 35 revealed that the selective growth of ZnO nanorod arrays on Si substrate and the mean diameters and lengths of the nanorods were in the range of 100 nm and 1 um, respectively. In Fig. 36, the ZnO nanorods show a clear hexagonal architecture on top for single crystal and a polycrystalline-like structure at the bottom. The grazing-angle XRD pattern of the nanorod was shown in Fig. 37. The positions of the main peaks in the grazing-angle XRD pattern were consistent with those of the hexagonal structure of bulk ZnO with lattice constants a_0 = 3.32489 A and c_0 = 5.2062A [159]. Besides, the polycrystalline were also shown in the pattern. As a result, the interface between ZnO nanorod and Si was not a perfect crystalline connection. To clarify the composition of the interface, EDX analysis was conducted and shown in Fig. 37. There is only Zn and O existed on the Si substrate.

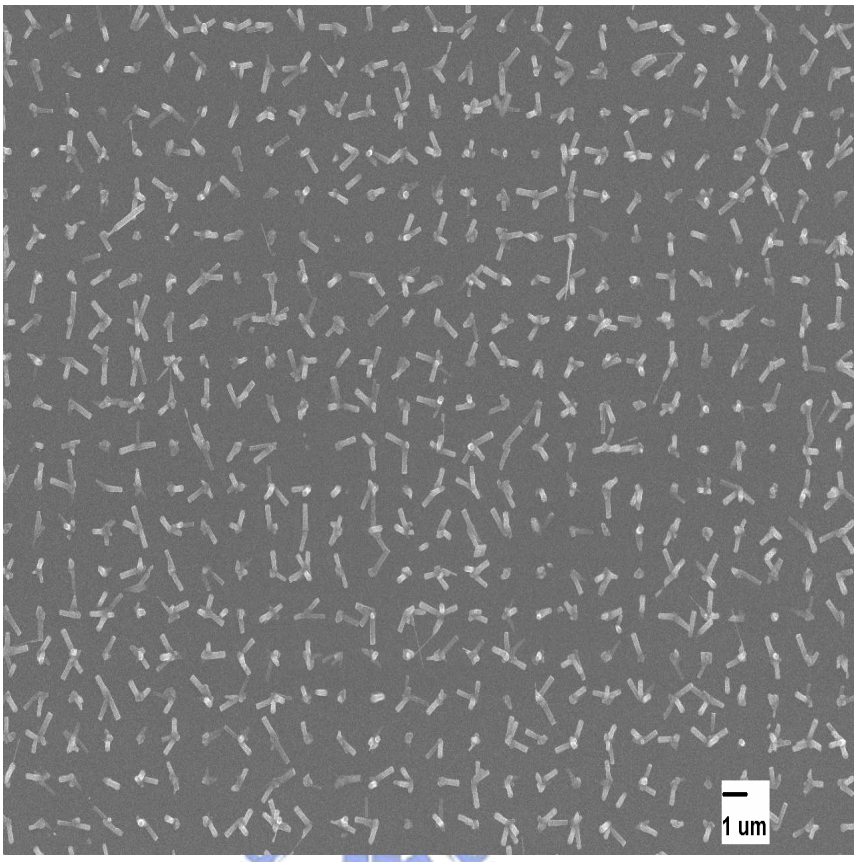

Fig. 35 SEM of selective growth of ZnO nanorod on Si substrate.

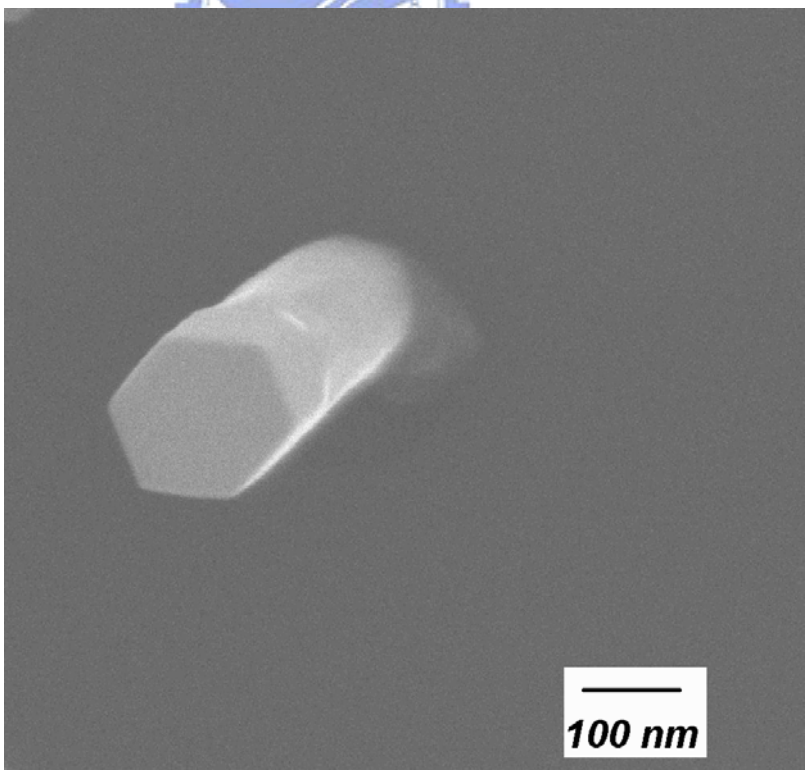

Fig. 36 Single ZnO nanorod with crystal structure on Si substrate.

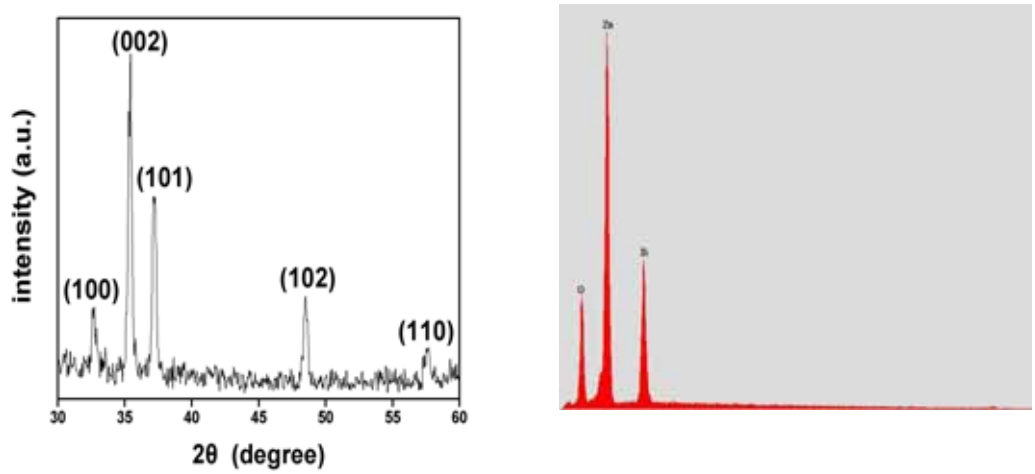

Fig. 37 The polycrystalline structure of ZnO nanorods and the evidence of only Zn and O element existed.

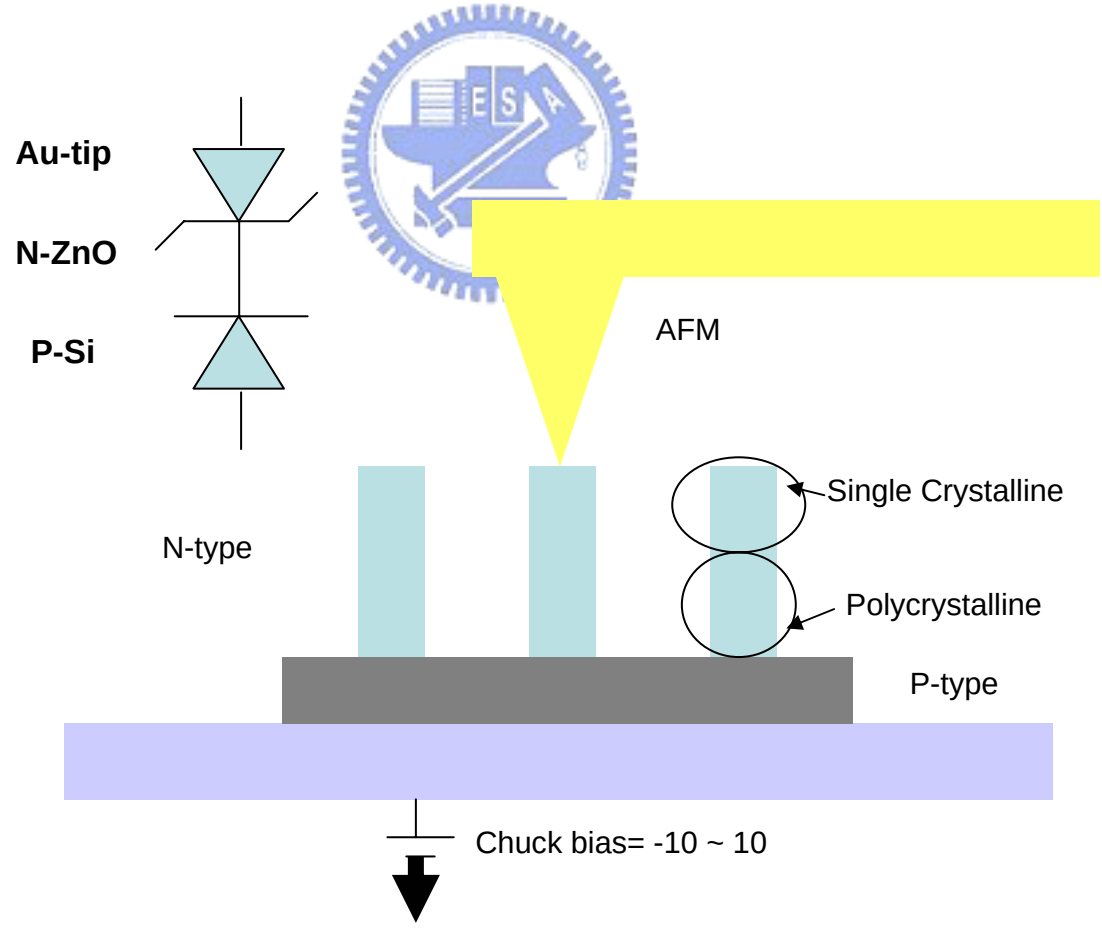

Fig.38 The AFM and SCM measurement setup

Fig. 38 shows the setup diagram for AFM and SCM. Prior to electrical characteristic measurements, the topography of ZnO nanorod arrays was obtained using an AFM. As shown in Fig. 39, the AFM image of a patterned ZnO nanorod array exhibits larger diameters of ZnO nanorods than those observed in SEM images. This distortion results from the tip convolution effect due to the high aspect ratio of the nanorods [177].

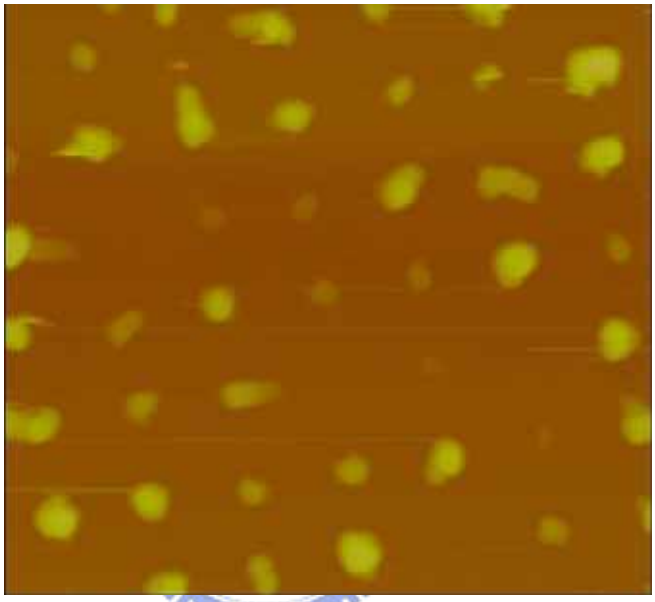

Fig. 39 The topography of ZnO nanorod using AFM.

5-3 I-V Results and Heterojunction

After the topography scanning, the AFM tip with an Au-coated tip was stopped on one single ZnO nanorod to obtain the current-voltage characteristic of the n-ZnO/p-Si and current-sensing AFM mode was carried out. The voltage is applied on the Si substrate and the current is detected on the tip terminal. The measured electrical characteristic in the Fig. 40 shows exponential dependence on the voltage in both sides. To explore the junction behavior, work function of ZnO nanorods and p-Si were obtained by Ultraviolet Photoelectron Spectrum. The work function

of ZnO nanorod was 5.2eV and was similar to that of ZnO nanobelts (5.2eV) and Au(5.3eV).[178]- [179] But the interface of metal Au and n-ZnO still showed a schottky contact[174]. The reason might be that the Fermi level is pinned at the ZnO surface. As a result, the ideality factors reported for the contaminated contact structures are routinely much larger than 1.

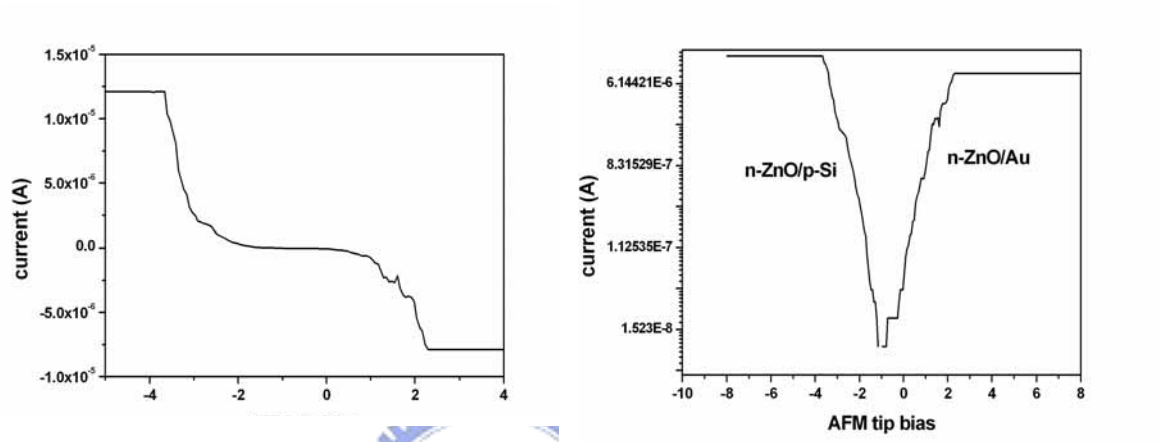

Fig. 40 The I-V characteristic of the n-ZnO/p-Si.

These two current are not probable response to the exponential increased current from the measurement. The current is dominated by the forward current of the ZnO/Si p-n junction. The diffused hole crossed the pn-junction are recombined with generated electrons at Au/ZnO junction. To maintain current continuity along the measurement loop, the generation rate at depletion area changed to exponentially since the generated electronics were recombined exponentially. The current-voltage was therefore explained by the pn-junction at forward bias as follows

$$J = J_s[\exp(\frac{eV}{nkT}) - 1]$$

Js is the reverse saturation current density, *k* the Boltzmann's constant, *T* is the absolute temperature, n is the ideality factor, V is the applied

voltage. The ideal factor, n is around 13.8 which means poor junction characteristics. This was consistent with our previous study [180], the ZnO nanorods are polycrystalline at ZnO/Si interface. Large defects account for the large ideal factor.

When the Au/n-ZnO/p-si under negative bias. The ZnO/Si junction was reverse biased at this moment. The only current is the reverse saturation current and the generation current from the depletion region of the junction. Either voltage independent or square-root dependence on the voltage as we described previously was satisfied. They do not response for the exponential dependence of the current-voltage characteristics. For the Au/ZnO junction, it is forward bias accordingly. The electron inject from ZnO to Au in a thermionic way. To fulfill the current continuity requirement, the electron generated exponentially from the depletion region since the electron across the schottky barrier exponentially. The current for schottky emission can be obtained by the equation:

$$J = A^{*}T^{2}\exp(\frac{-e\phi_{Bn}}{kT})[\exp(\frac{eV}{nkT})-1]$$

A* is the Richardson constant, k the Boltzmann's constant, φ_{Bn} is the Schottky barrier height; T is the absolute temperature, n is the ideality factor, V is the applied voltage. The ideal factor, n is around 11 much better than the ZnO/Si junction indicates better ZnO quality. This can understood from the Fig.1, the AFM image shows single crystal-like hexagonal structure. However, this value is still a little higher than other group [174]. This is attributed to the non-perfect contact between Au tip and ZnO nanorod during the experiment.

Base on the work function measurement, the band diagram of Au/n-ZnO/p-Si is discussed. At positive applied voltage, the p-Si/n-ZnO pn-junction was forward biased while Au/n-ZnO schottky was reversed

biased. Under forward bias, the holes diffuse across the pn junction from the p-type Si into n-type ZnO and from ZnO to Si for electronics. For the Au/ZnO junction, reverse bias causes the depletion region increased with the increase of the bias. The current at this junction are mainly from the reverse electron leakage current from Au to ZnO and the generation current in the depletion region. Therefore, negative current was detected. The junction leakage current is independent to the applied voltage and solely depends on the barrier height between Au and ZnO as well as the temperature. The generation current is linearly depends on the depletion width. The depletion width has square-root dependence on the voltage.

5-4 C-V Discussions and Interface state

The equal electric circuit diagram is shown in Fig. 41. There were two opposite diodes with series connection, one is Schottky diode and the other is Heterojunction diode. The capacitance of Schottky contact, Cjm, is from the depletion region in the junction. And the diffusion and junction capacitances, Cdh and Cjh respectively, were formed with parallel connection in the Heterojunction.

Before the C-V measurement, we have calibrated our SCM system with a known sample. When this negative bias was applied on Au-coated tip, the forward bias was formed in the Heterojunction contact as shown in Fig. 42. At low voltage, the total capacitance came from the series-parallel connection of Cjm, Cjh and Cdh. Cdh was larger than Cjh as increasing voltage, the total capacitance became the series connection between Cjm and Cdh. As a result, we measured the Cjm with high voltage.

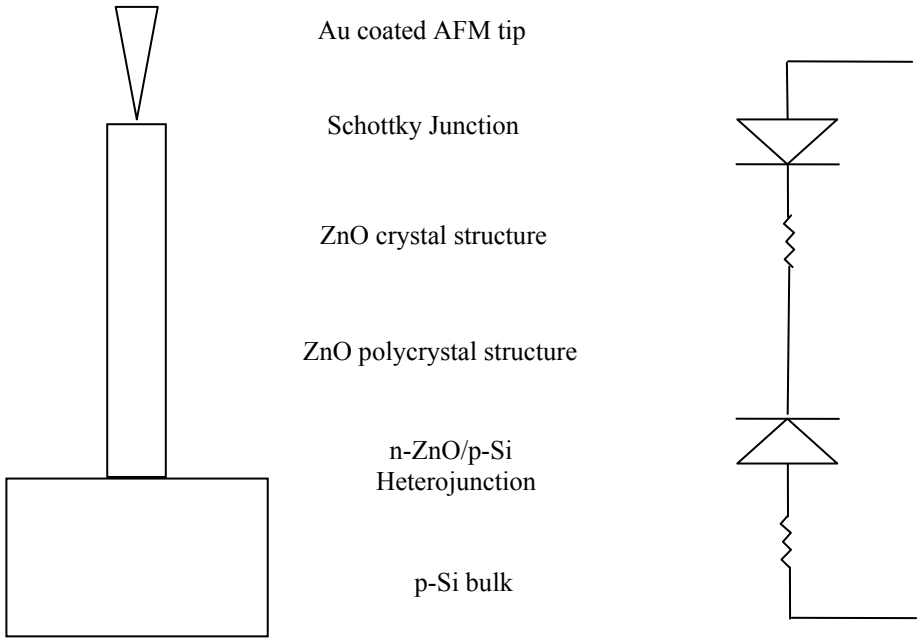

Fig. 41 Equal electric circuit diagram of the single n-ZnO nanorod measured by conductive AFM.

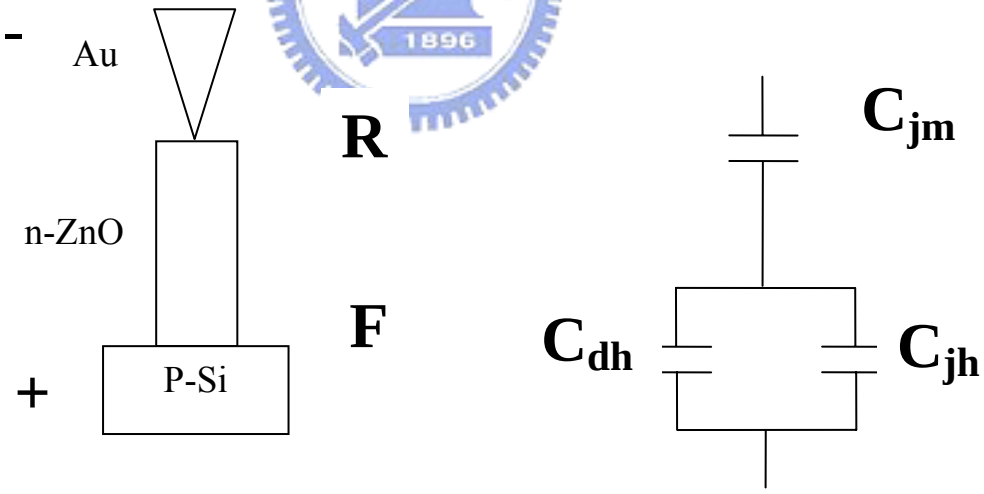

Fig. 42. Negative bias applied on Au-coated tip and the series-parallel connection of Cjm, Cjh and Cdh.

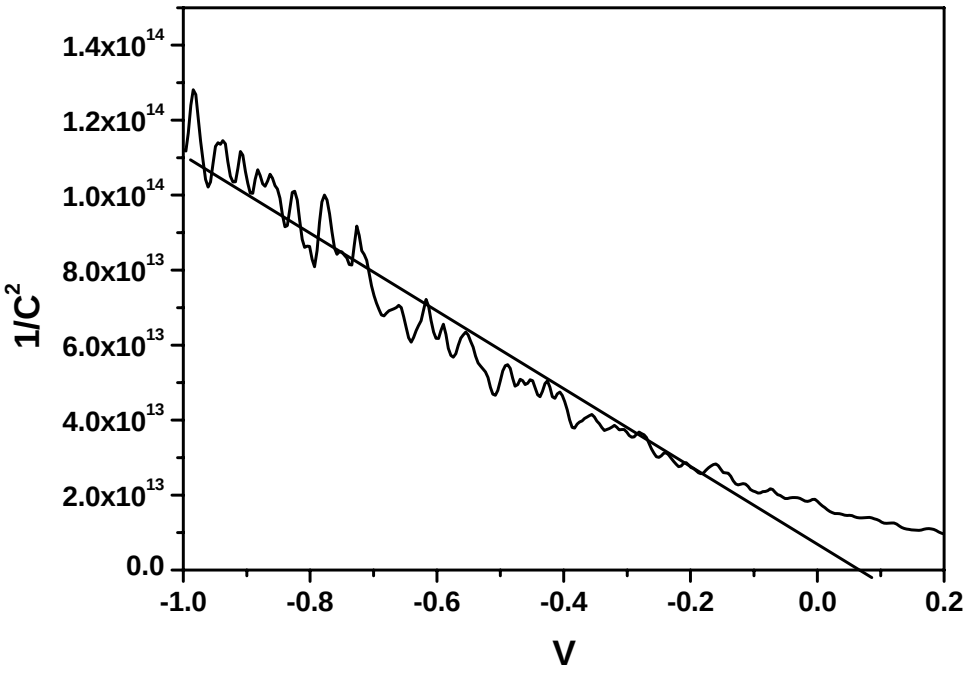

Fig. 43 The $1/C^2$-V curve of the Schottky junction.. From the slope and the intercept, the concentration of n-ZnO nanorod and the built-in voltage were calculated respectively.

The 1/C2-V curve was plotted in Fig. 43. From the slope and the intercept of the Schottky junction(one-side abrupt junction), the concentration of n-ZnO nanorod and the built-in voltage V_{bim} were calculated respectively. The calculation was as followed:

Schottky junction width $W = \sqrt{\frac{2\varepsilon_s(V_{bi} - V_R)}{qN_B}}$

The capacitance per area $C_{jm} = \frac{\varepsilon_s}{W} = \sqrt{\frac{q\varepsilon_s N_B}{2(V_{bi} - V_R)}}$

$$(\frac{1}{C_{jm}})^2 = \frac{2(V_{bi} - V_R)}{q\varepsilon_s N_B}$$

And we had $\varepsilon_{ZnO} = 8$ $\varepsilon_0 = 8.85E-14$ (F/cm) from the literature [181] The contact area was estimated about 3.14*50nm*50nm.Then the concentration of n-ZnO is N_{ZnO} = 1.76E17. And we assume the

concentration was the same in the ZnO nanorod. The built-in voltage was about 0.043 V and the Schottky barrier height (ϕ_{Bn}) was calculated as followed:

V_{bim}=0.08

$\phi_n = \frac{kT}{e}\ln(\frac{N_c}{N_d})$=0.267 Nc of ZnO = 2.964E18 (me*=0.24)

$V_{bim} = \phi_{Bn} - \phi_n$

ϕ_{Bn} = 0.08+0.267=0.347 eV

The Schottky barrier height calculation was consistent from the C-V and I-V measurements. The discussed I-V equation was listed here:

$J = J_{st}[\exp(\frac{eV_a}{nkT}) - 1]$

$J_{st} = A^*T^2 \exp(\frac{-e\phi_{Bn}}{kT})$

ϕ_{Bn} = 0.35 eV

$J = 0.1217A^* \exp(\frac{V}{0.0259n} - 1)$

On the contrary, when this negative bias was applied on the p-Si substrate, the forward bias was formed in the Heterojunction contact as shown in the Fig. 44. At low voltage, the total capacitance came from the series-parallel connection of Cjm, Cjh and Cdh. Cdh was little and Cjh was increased as increasing voltage. The total capacitance became the series connection between Cjm and Cjh. Finally, we found that the Cjh dominated the capacitance. The measurement curve was shown in Fig. 45. In order to calculate the band diagram discontinuity, we have to know the doped-concentration of p-Si. The resistivity of our p-Si substrate is about 1~100 (Ω-cm) and we measured the work function from UPS is about 4.7~4.8 (eV.)

We calculated the work function of p-Si with the following equations: The slope of the 1/C2-V curve is 5E16

$$C_{jh}^{\ 2} = \frac{qN_D N_A \varepsilon_{ZnO}\varepsilon_{Si}}{2(N_A\varepsilon_{ZnO} + N_D\varepsilon_{Si})} \frac{1}{(V_{bi}+V)} = \frac{2}{(1.6E-19)*8*(8.85E-14)*N_{Si}} = 5E16$$

N_{Si}=3.5E14(cm3)

$E_F - E_V = kT\ln(\frac{N_V}{N_A})$ N_V=1.04E19 (cm-3)

Work function of p-Si was about 4.83 eV and it was also an one-side abrupt junction

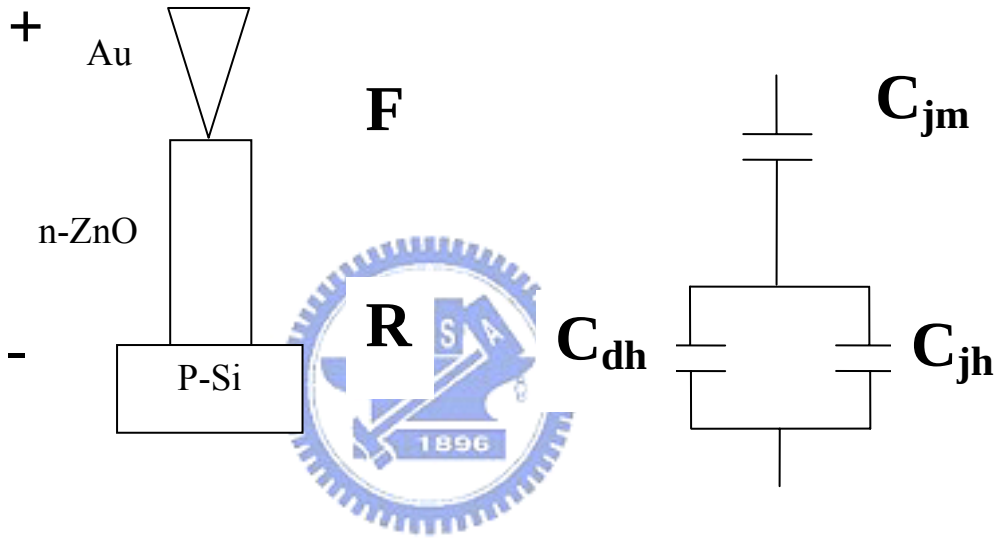

Fig. 44 Negative bias applied on p-Si substrate and the series -parallel connection of Cjm, Cjh and Cdh.

The work function of our ZnO nanorod was measured by UPS and compared with the literatures as shown in the Table 5. We determine it is 5.3 eV and the band diagram was shown in Fig. 46 : before contact and after contact.

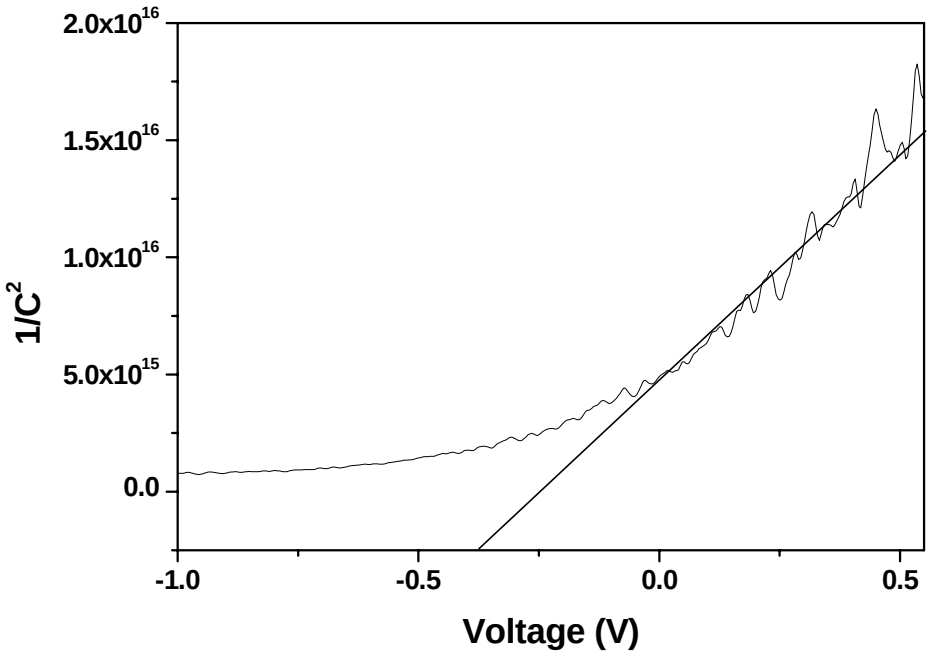

Fig. 45 The $1/C^2$-V curve of Heterojunction. From the slope and the intercept, the concentration of p-Si and the V_{bi} were found.

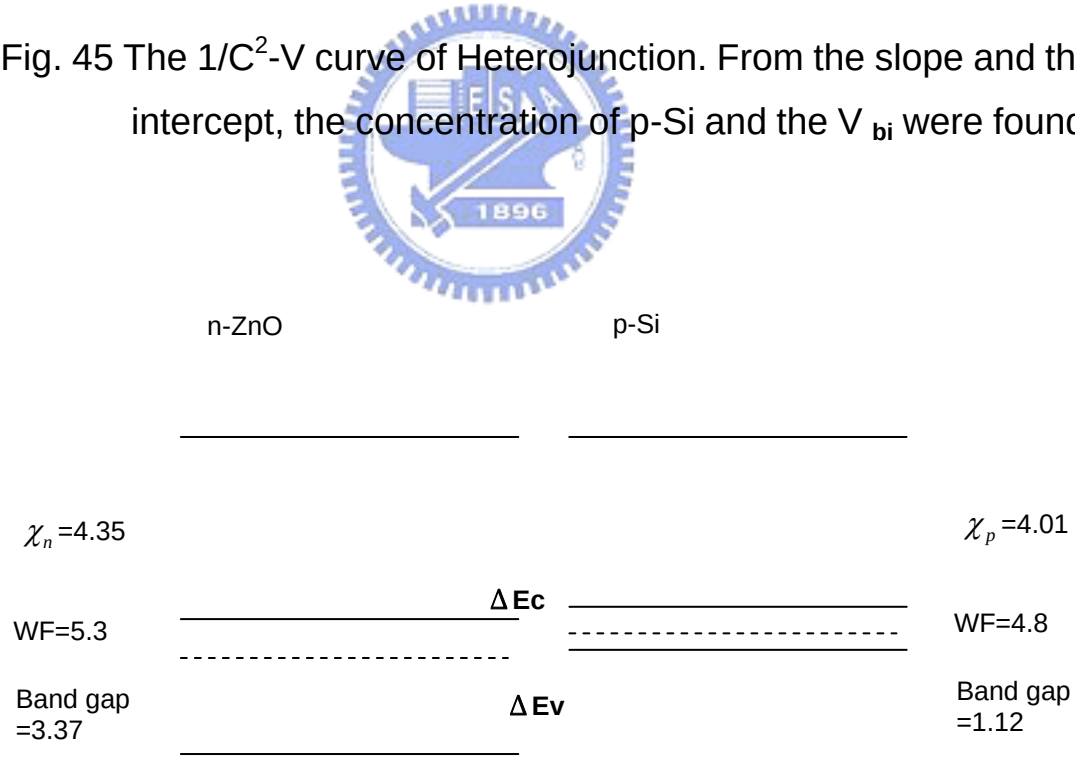

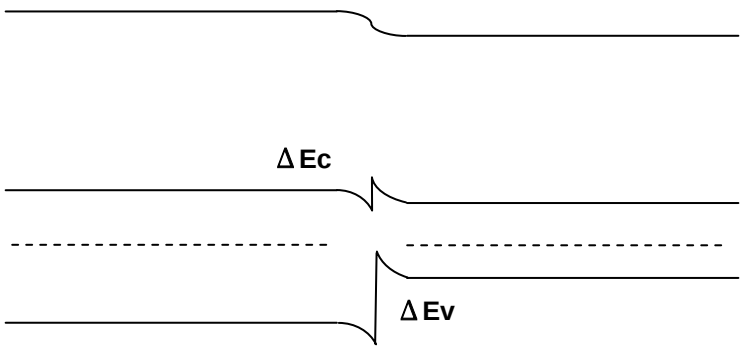

Fig. 46 The heterojunction of n-ZnO/p-Si band diagram before and after contact.

ZnO WF (eV)	Film or Nano	Method / Literature	Application	ref
4.25	Film	Literature Assume	Heterojunctionn	[182]
4.25	Film	Literature Assume	Sol-Gel	[183]sited[182]
4.45~4.5	Film	IV Calculated	Heterojunctionn	[184]
5.2	Nanobelt	TEM	electrochemical	[185]
5.3	Film	UPS	Alloy change	[186]
5.3	Nanowire	Literature	Field Emission	[187]sited[186]
4.5	Film	Literature assume	Photodiode Diagram	[188]
4.5	Film	Literature assume	Photodiode Diagram	[189]
5.3	Nanowire	Calculated	Field Emission	[190]sited[186]
5.3	Nanorod	UPS	Field Emission	ours

TABLE 5. work function list of ZnO from literature

V_{Bih}=-0.37 from the intercept of slope

The relation of V_{Bi}, the intercept of C-V slope, and ΔE_C was calculated as followed:

$$eV_{bih} = \phi_{sn} - \phi_{sp}$$

$$= [e\chi_n + (E_{Cn} - E_{Fn})] - [e\chi_p + E_{gp} - (E_{Fp} - E_{Vp})]$$

$$= e(\chi_n - \chi_p) + (E_{Cn} - E_{Fn}) + (E_{Fp} - E_{Vp}) - E_{gp}$$

$$= \Delta E_C + (kT \ln \frac{N_{Cn}}{n_{on}}) + (kT \ln \frac{N_{Vp}}{P_{op}}) - E_{gp}$$

$$= \Delta E_C + kT \ln(\frac{N_{Cn} N_{Vp}}{n_{on} P_{op}}) - E_{gp}$$

-0.37= ΔE_C +0.34-1.12

where

$E_{gp} = 1.12eV, N_{Cn} = 2.694E18, N_{Vp} = 1.04E19, n_{on} = 1.76E17, P_{op} = 3.5E14$

$\Delta E_C = 0.41eV$

and from I-V measurement

$$J = \frac{qA^* T^2 V_{bi}}{kT} \exp(\frac{-qV_{bi}}{kT})(1 - \frac{V}{V_{bi}})[\exp(\frac{qV}{kT}) - 1]$$

$$J = J_0 (1 - \frac{V}{V_{bi}})[\exp(\frac{qV}{kT}) - 1]$$

$$J \propto A^* T^2 \exp(\frac{-E_w}{nkT})$$

E_w =0.33 eV

The ΔE_C calculation of heterojunction barrier from the C-V method was similar to the energy barrier height from I-V measurement. From the band diagram,

$$\Delta E_C + E_{gZnO} = \Delta E_V + E_{gSi}$$

$$\Delta E_g = E_{gZnO} - E_{gSi} = \Delta E_V - \Delta E_C$$

$$\Delta E_V = \Delta E_g + \Delta E_C$$

ΔE_V = (3.37-1.12)+0.4=2.65 eV

Without consider Interface States in heterojunction, for heterojunction at constant temperature, Cdh and Cjh was known as:

$$C_{dh} = C_d = \frac{AdQ_p}{dV} = \frac{Aq^2 L_p P_{no}}{kT} e^{\frac{qV}{kT}}$$

$$C_{dh} = C_d = \frac{1}{2V_t}\left(I_{po}\tau_{po} + I_{no}\tau_{no}\right)$$

$$L_p^{\ 2} = D_p \tau_{po}$$

$$Cd = \frac{q}{KT}\left(\frac{qLpPno}{2} + \frac{qLnNpo}{2}\right)\exp\left(\frac{qVo}{KT}\right)$$

$$Cd = A\exp(BVo)$$

$$C_{jh}^{\ 2} = \frac{qN_D N_A \varepsilon_{ZnO}\varepsilon_{Si}}{2(N_A\varepsilon_{ZnO} + N_D\varepsilon_{Si})}\frac{1}{(V_{bi} + V)}$$

$$C_{jh} = Cj = \sqrt{\frac{qN_D N_A \varepsilon_1 \varepsilon_2}{2(N_A\varepsilon_1 + N_D\varepsilon_2)(V + V_{bi})}}$$

But if consider interface state, Cjh become the following equation [191]-[192]

$$Cjh = \left[\frac{2q\varepsilon_1\varepsilon_2 N_D N_A}{\varepsilon_1 N_A + \varepsilon_2 N_D}\right]^{\frac{1}{2}}(V_{bi} - V - B_2 Q_2)^{\frac{-1}{2}}\left[1 + f(V)\frac{dQs}{dV}\right]$$

Where Q_S is the interface charge, $f(V)$ is a V-dependent function and B_2 is a constant depends on N_A and N_D. Theoretically, the built-in voltage in an ideal contact is about 0.66 eV and the intercept of our data is 0.37. As a result,

$$B_2 Q_2^{\ 2} = 0.29$$

First, we assume interface charge is independent of applied voltage $f(V)=0$

$$C_{jh} = \left[\frac{2q\varepsilon_1\varepsilon_2 N_D N_A}{\varepsilon_1 N_A + \varepsilon_2 N_D}\right]^{\frac{1}{2}}(0.66 - V - B_2 Q_s^{\ 2})^{\frac{-1}{2}}$$

When $N_D >> N_A$

$$C_{jh} = [2q\varepsilon_1 N_A]^{\frac{1}{2}}(0.66 - V - B_2 Q_s^{\ 2})^{\frac{-1}{2}}$$

$$Cj = [2*1.6E-19*8*8.85E-14*3.5E14]^{\frac{1}{2}}(0.66-V-B_2Q_s{}^2)^{\frac{-1}{2}}$$

$$Cj = 8.9E-9*(0.66-V-B_2Q_s{}^2)^{\frac{-1}{2}}$$

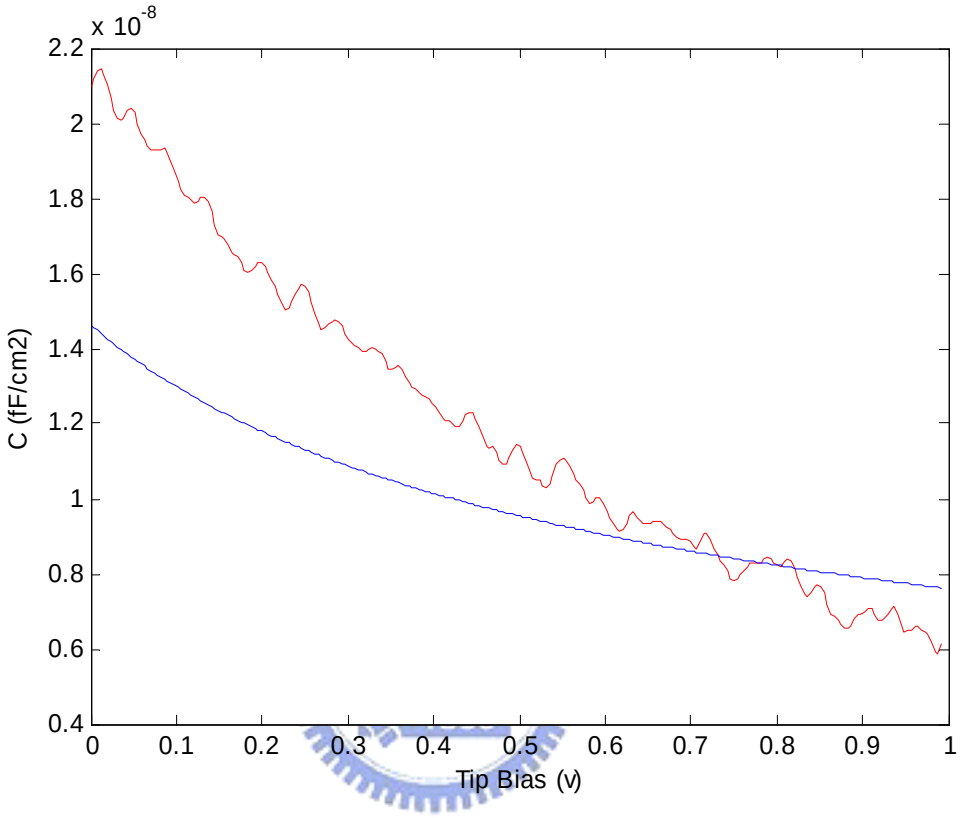

Fig. 47 The disagreement of C-V curve from measured (red) and calculated (blue) data. We assumed that the interface state was independent of applied voltage.

The difference curves between the measured data and the assumed data was shown in Fig. 47, the assumption might be incorrect. The interface state might be affected by the applied voltage. Therefore the simplified equation must be corrected.

Second, we assume interface charge is dependent of applied voltage

$$Cjh = [\frac{2q\varepsilon_1\varepsilon_2 N_D N_A}{\varepsilon_1 N_A + \varepsilon_2 N_D}]^{\frac{1}{2}}(V_{bi} - V - B_2Q_2)^{\frac{-1}{2}}[1 + f(V)\frac{dQs}{dV}]$$

$$V_{bi} = V_{bih}(ideal) = 0.66 \quad (\text{eV})$$

$$B_2 Q_2^{\ 2} = 0.29$$

$$f(V)\frac{dQ_s}{dV} = -0.6775V + 0.5$$

And the fitting curve is shown in Fig. 48. From the overlap fitting curve, interface state might be considered and it was dependent of applied voltage.

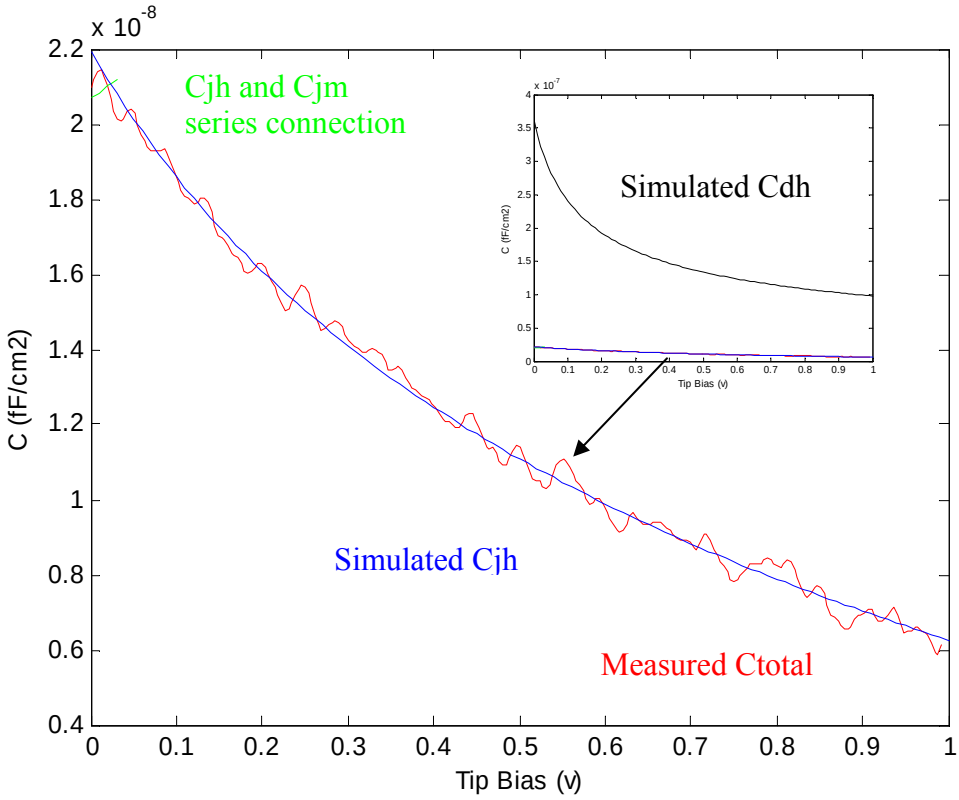

Fig. 48 The agreement of C-V curve from measured (red) and calculated (blue) data. We assumed that the interface state was dependent of applied voltage.

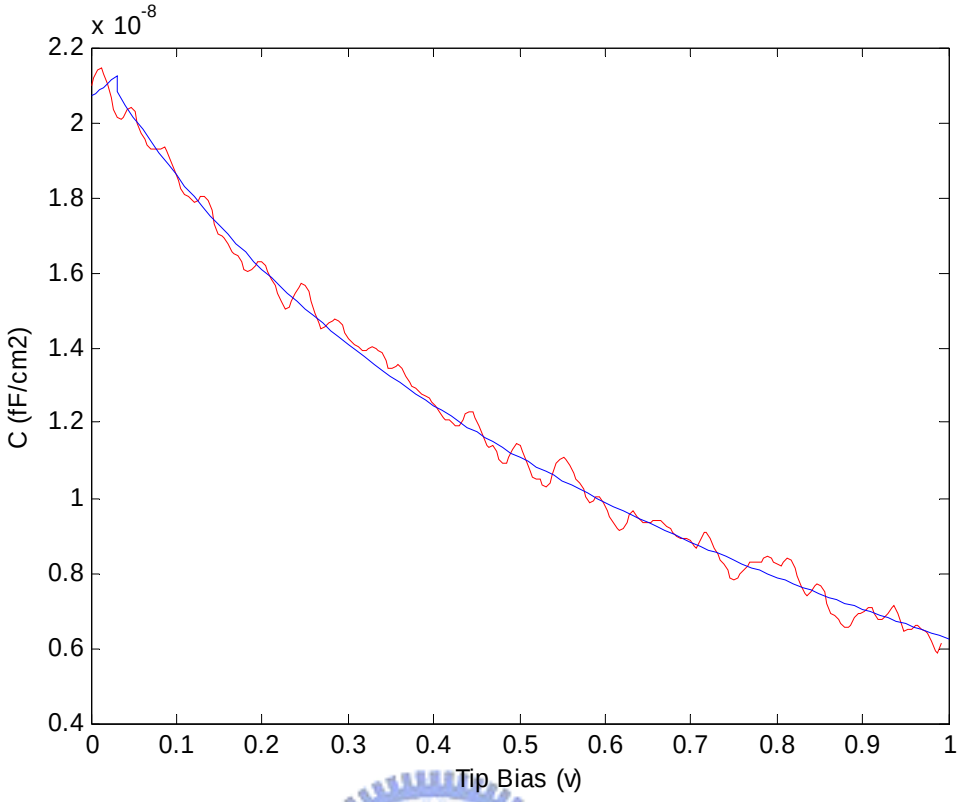

Fig. 49 The C-V curve from measured (red) and calculated (blue) data. The series connection of Cjm and Cjh was carried out at low voltage below 0.08V.

The parallel connection between Cjm and Cjh at low voltage was shown in Fig. 49. We found that the voltage ratio of Cjm and Cjh was -0.9V : -0.1V and the capacitance was contributed from the charges in the heterojunction when the reverse bias was applied on p-Si substrate and the voltage-dependent interface state was necessary considered.

When the native bias was applied on the Au-coated tip, on the other hand, we use the same equation of Cjh for the series connection with Cjm to fit the measured data.

The fitting and measured curves were showed in Fig. 50 and it is quite match. We found that the series connection of Cjh and Cjm contributed the capacitance and Cdh contributed little at low voltage. As the voltage increasing, Cjm dominated the capacitance.

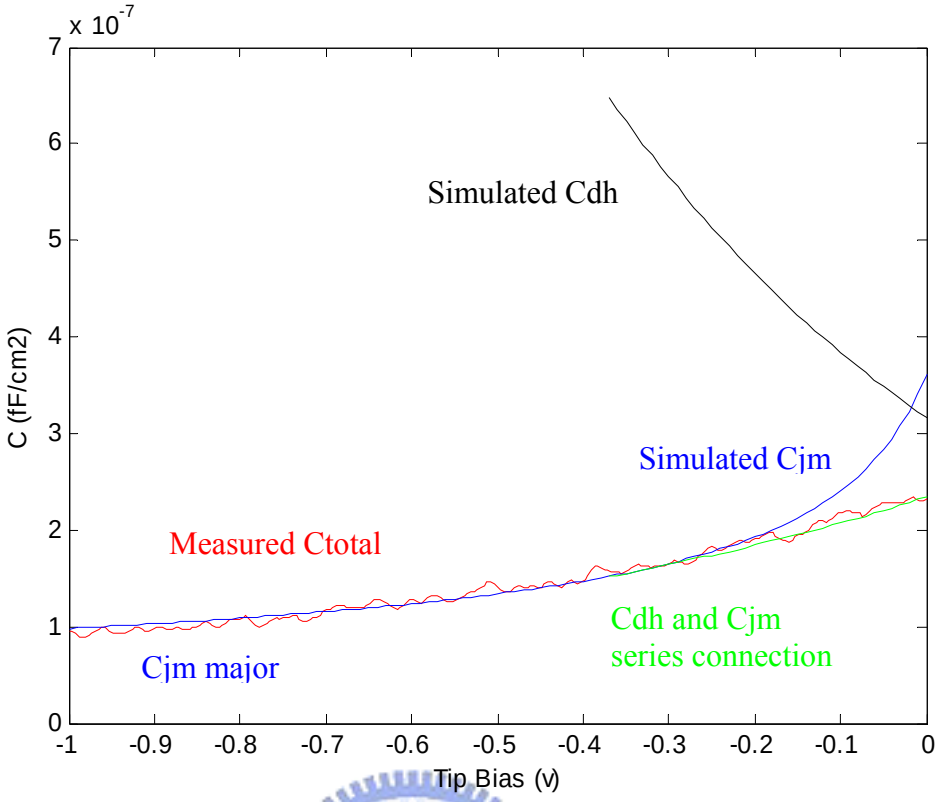

Fig. 50 The C-V curve from measured (red) and calculated (green and blue) data. the series connection of Cdh and Cjm contributed the capacitance at low voltage. Cjm dominated at high voltage.

For 0~-0.37V, the Cjh was smaller than the Cdh and they were in parallel connection then series with Cjm. As a result, Cdh and Cjm contributed the capacitance and the voltage consumed ratio was 0.85V : 0.15V. But for -0.37~-1V, the Cdh was increased and larger than Cjm and they are in series connection. The capacitance was certainly contributed mainly by the charge in the Schottky junction. Finally, the discontinuity of band structure with interface state was shown on Fig. 51.

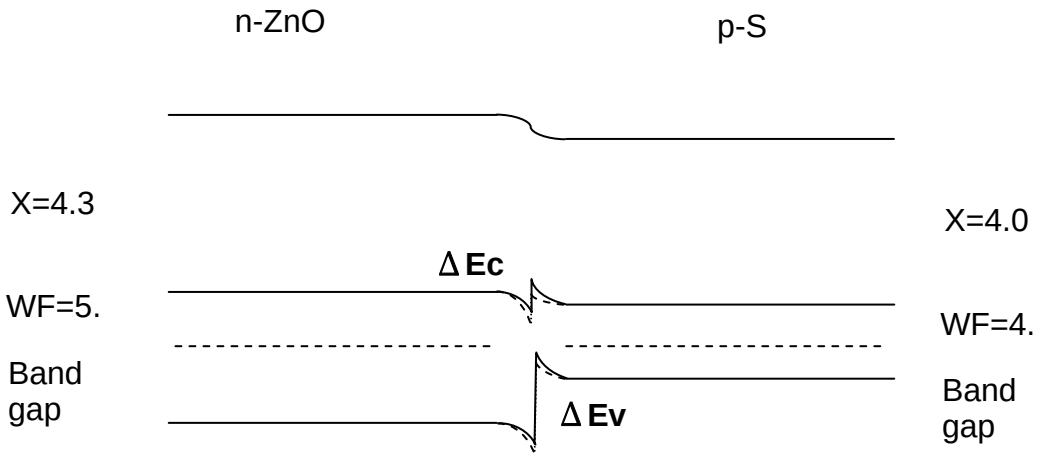

Fig. 51 The correction of heterojunction of n-ZnO/p-Si band diagram considering the interface state.

And the interface states density σ can be calculated from the Vbi

$$V_{bi} = \frac{qN_A}{2\varepsilon_1}\chi_j^{\,2} + \frac{qN_D}{2\varepsilon_2}(W-\chi_j)^2 + \frac{qND}{\varepsilon_1}(W-\chi_j)\chi_j - \frac{q\sigma\chi_j}{\varepsilon_1}$$

Vbi(ideal)-Vbi(with interface charge)=$\frac{q\sigma\chi_j}{\varepsilon_1}$

Where q=1.6E-19, $\varepsilon_1 = \varepsilon_{ZnO} = 8 \quad \varepsilon_0 = 8.85E-14$ (F/cm)

χ_j=depletion width inside p-Si

$$\chi_j = \{\frac{2\varepsilon_1 V_{bi}}{q}[\frac{N_D}{N_A}][\frac{1}{N_D+N_A}]\}^{\frac{1}{2}}$$

$$= \{\frac{2\varepsilon_n\varepsilon_p N_D V_{bi}}{qN_A(\varepsilon_n N_D + \varepsilon_p N_A)}\}^{\frac{1}{2}}$$

When $N_D >> N_A$

$$\chi_j = \{\frac{2\varepsilon_1 V_{bi}}{qN_A}\}^{\frac{1}{2}} = \{\frac{2*12*8.85E-14*0.5}{1.6E-19*3.5E14}\}^{\frac{1}{2}} = 1.377\text{E-4cm} = 1.377\text{um}$$

$$0.66-0.48(eV) = \frac{1.6E-19(q)*\sigma*1.377E-4(cm)}{12*8.85E-14(F/cm = q/eV*cm)}$$

σ=8.676E9(cm-2)

As a result, the density of interface state is about 9E9 per cm square.

In the end, we calculated the frequency response of the two junctions:

schottky and heterojunction as shown in Fig. 52 and they are GHz and MHz, respectively. The totally FED operated speed is controlled by the heterojunction.

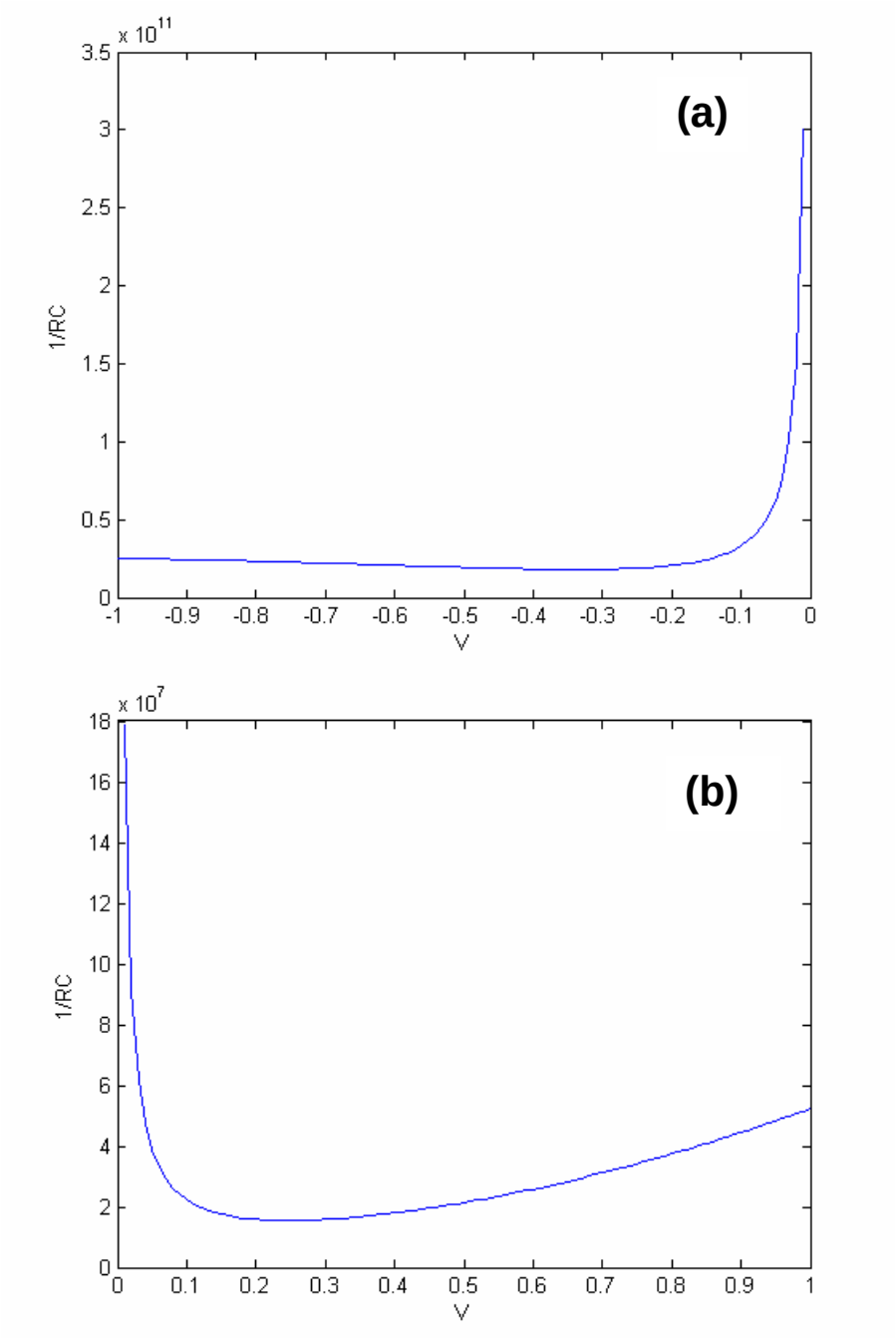

Fig. 52 The frequency response of Schottky junction (a) and heterojunction (b).

5-5 Conclusion

We measured the electric properties of single ZnO nanorod by conductive AFM and SCM. From those measurements, the schottky barrier height was about 0.34 eV and the ideal factor was about 11 due to the contact resistance and series connection of resistance from ZnO nanorod. The ΔE_C of heterojunction was also about 0.4 eV and the built-in voltage was about 0.37 eV below the ideal contact resulting from the interface state existing. The interface between n-ZnO nanorod and p-Si was existed. The frequency response of the schottky junction was GHz scale but MHz for heterojunction. As a result, the operated frequency of the FED composed from single ZnO nanorod and p-Si was only MHz scale.

Appendix

From Poisson's equation

$$dE = \frac{dQ}{\varepsilon_s} \qquad Cj = \frac{dQ}{dV} = \frac{dQ}{WdE} = \frac{dQ}{W\frac{dQ}{\varepsilon_s}} = \frac{\varepsilon_s}{W}(F/cm^2)$$

For metal-semiconductor Cjm

$$Cj = \sqrt{\frac{q\varepsilon_s N_B}{2(V_{bi}-V)}} = \frac{1E-7}{\sqrt{(0.08-V)}}$$ **(after simulation Cjm=1.02*** $\frac{1E-7}{\sqrt{(0.08-V)}}$ **)**

For heterojunction Cd

$$Cd = \frac{q}{KT}(\frac{qLpPno}{2} + \frac{qLnNpo}{2})\exp(\frac{qVo}{KT})$$

$$Cd = A\exp(BVo)$$

$$Cd = A\exp(\frac{V-0.37}{0.0259n})$$ **A=0.0000015, n=17**

For heterojunction Cjh

assume $f(V)$=0

$$Cj = [\frac{2q\varepsilon_1\varepsilon_2 N_D N_A}{\varepsilon_1 N_A + \varepsilon_2 N_D}]^{\frac{1}{2}}(0.5 - V - B_2Q_s{}^2)^{\frac{-1}{2}}$$

When $N_D >> N_A$

$$Cj = [2q\varepsilon_1 N_A]^{\frac{1}{2}}(0.66 - V - B_2Q_s{}^2)^{\frac{-1}{2}}$$

$$Cj = [2*1.6E-19*8*8.85E-14*3.5E14]^{\frac{1}{2}}(0.66 - V - B_2Q_s{}^2)^{\frac{-1}{2}}$$

$$Cj = 8.9E-9*(0.66 - V - B_2Q_s{}^2)^{\frac{-1}{2}}$$

assume $f(V)$ exist

$$Cjh = [\frac{2q\varepsilon_1\varepsilon_2 N_D N_A}{\varepsilon_1 N_A + \varepsilon_2 N_D}]^{\frac{1}{2}}(V_{bi} - V - B_2Q_2)^{\frac{-1}{2}}[1 + f(V)\frac{dQs}{dV}]$$

$$V_{bi} = V_{bih}(ideal) = 0.66 \quad (\text{eV})$$

$$B_2Q_2{}^2 = 0.29$$

$$f(V)\frac{dQ_s}{dV} = -0.6775V + 0.5$$

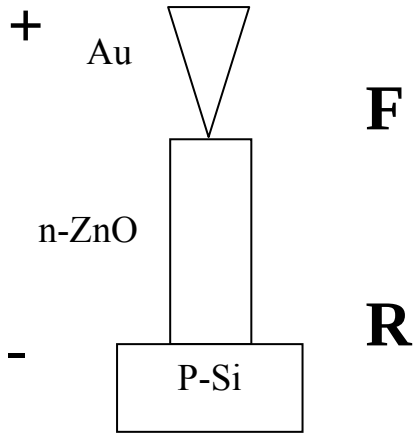

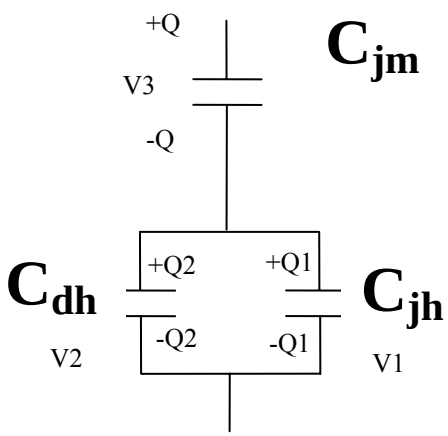

Cjh*V1=Q1

Cdh*V2=Q2

V1=V2

Cjh*V1+ Cdh*V2=Q1+Q2=Q=Cjm*V3

V1+V3=Vapplied

With curve fitting of total capacitance, partial voltage of each capacitance can be found.